Inorganic Chemistry

Article

pubs.acs.org/IC

Phosphazene Based Multicentered Naked-Eye Fluorescent Sensor with High Selectivity for Fe^{3+} Ions

Reyhan Kagit,[†] Mehmet Yildirim,[‡,§] Ozgur Ozay,[∥] Serkan Yesilot,[⊥] and Hava Ozay*[,†]

[†]Department of Chemistry, Inorganic Chemistry Laboratory, Faculty of Science and Arts, Canakkale Onsekiz Mart University, Canakkale 17020, Turkey

[‡]Department of Materials Science and Engineering, Faculty of Engineering, Canakkale Onsekiz Mart University, Canakkale 17020, Turkey

[§]Department of Chemistry, Polymer Synthesis and Analysis Laboratory, Faculty of Science and Arts, Canakkale Onsekiz Mart University, Canakkale 17020, Turkey

[∥]Lapseki Vocational School, Department of Chemistry and Chemical Processing Technologies, Canakkale Onsekiz Mart University, Lapseki/Canakkale 17800, Turkey

[⊥]Department of Chemistry, Gebze Institute of Technology, Gebze/Kocaeli 41400, Turkey

Supporting Information

ABSTRACT: A novel on/off fluorescent rhodamine-based hexapodal Fe^{3+} probe (**L**) containing a cyclotriphosphazene core was synthesized by an azide−alkyne "click-reaction". The synthesized compounds (**1**−**5** and **L**) were characterized by FT-IR; ^{1}H, ^{13}C, and ^{31}P NMR; and MALDI MS spectrometry. The optical sensor features for the Fe^{3+} complex of **L** were investigated by UV−vis and fluorescence spectroscopy. The stoichiometry of **L**−Fe^{3+} complex was found to be 1:3 (ligand/metal ion), and the detection limit of **L** was determined as 4.8 μM (0.27 mg L^{-1}) for Fe^{3+} ions. The reusability of the sensor was tested by the addition of ethylenediamine to **L**−Fe^{3+} complex solutions followed by the addition of Fe^{3+} solution.

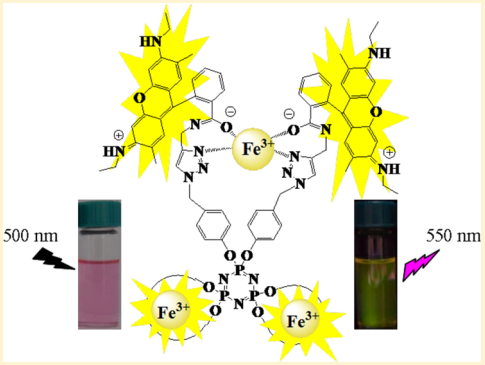

INTRODUCTION

Phosphazene compounds, which are characterized by the double bond in between phosphorus and nitrogen atoms, comprise a large class of inorganic compounds.[1−5] These compounds have been the center of interest for many researchers, as halogen atoms bound by phosphorus atoms in their structure may easily undergo a substitution reaction with nucleophilic compounds. The vast majority of studies relevant to phosphazenes are based on substitution reactions of these compounds with nucleophilic compounds such as amines, alcohols, and phenols.[6−8] Some phosphazene derivatives and polymers have applications in various industrial and medical areas such as the production of inflammable textile fibers and elastomers,[9] liquid crystals,[10] anticancer[11] and antibacterial reagents,[12] synthetic bone and inert biomaterials for tissue engineering,[13,14] and multicenter coordination compounds.[15] In addition to this, the cyclic phosphazenes are interesting compounds as a core for the synthesis of dendrimeric structures due to substituted groups on phosphorus atoms positioned above and below the plane of the phosphazene ring.[8,16−18] Therefore, phosphazene compounds are a very interesting class of inorganic−organic hybrid compounds.

Detection of heavy metals by optical methods has been favored due to their relatively lower cost compared to instrumental methods such as inductively coupled plasma atomic emission or mass spectroscopy (ICP-AES, ICP-MS), atomic absorption spectroscopy (AAS), etc. For this reason, several studies have focused on construction of selective, sensitive and reversible ion sensors using spectral methods. Both spectrophotometric and spectrofluorometric methods are available for optical chemosensors.[19,20] These sensing applications generally depend on quenching/growing of emission or absorption peaks. Fluorescence signaling supplies high sensitivity and easy handling as well as being cheaper to use. Many studies have been carried out to decrease the detection limits while generating high selectivity. Development of a new generation of optical sensors is still needed for environmental and biological requirements. The Fe^{3+} ion in the structure of many enzymes is involved as a catalyst for oxygen metabolism and electron transfer mechanisms in the human body.[21,22] However, a high concentration of Fe^{3+} ions has a toxic effect on living organisms and causes diseases such as Parkinson's disease and Alzheimer's disease.[23,24] Therefore, a few colorimetric sensors have been developed for this iron ion species. Rhodamine derivatives are the most common among these

Received: November 6, 2013
Published: February 5, 2014

   dx.doi.org/10.1021/ic402783x | *Inorg. Chem.* 2014, 53, 2144−2151

Scheme 1. Synthesis of L[a]

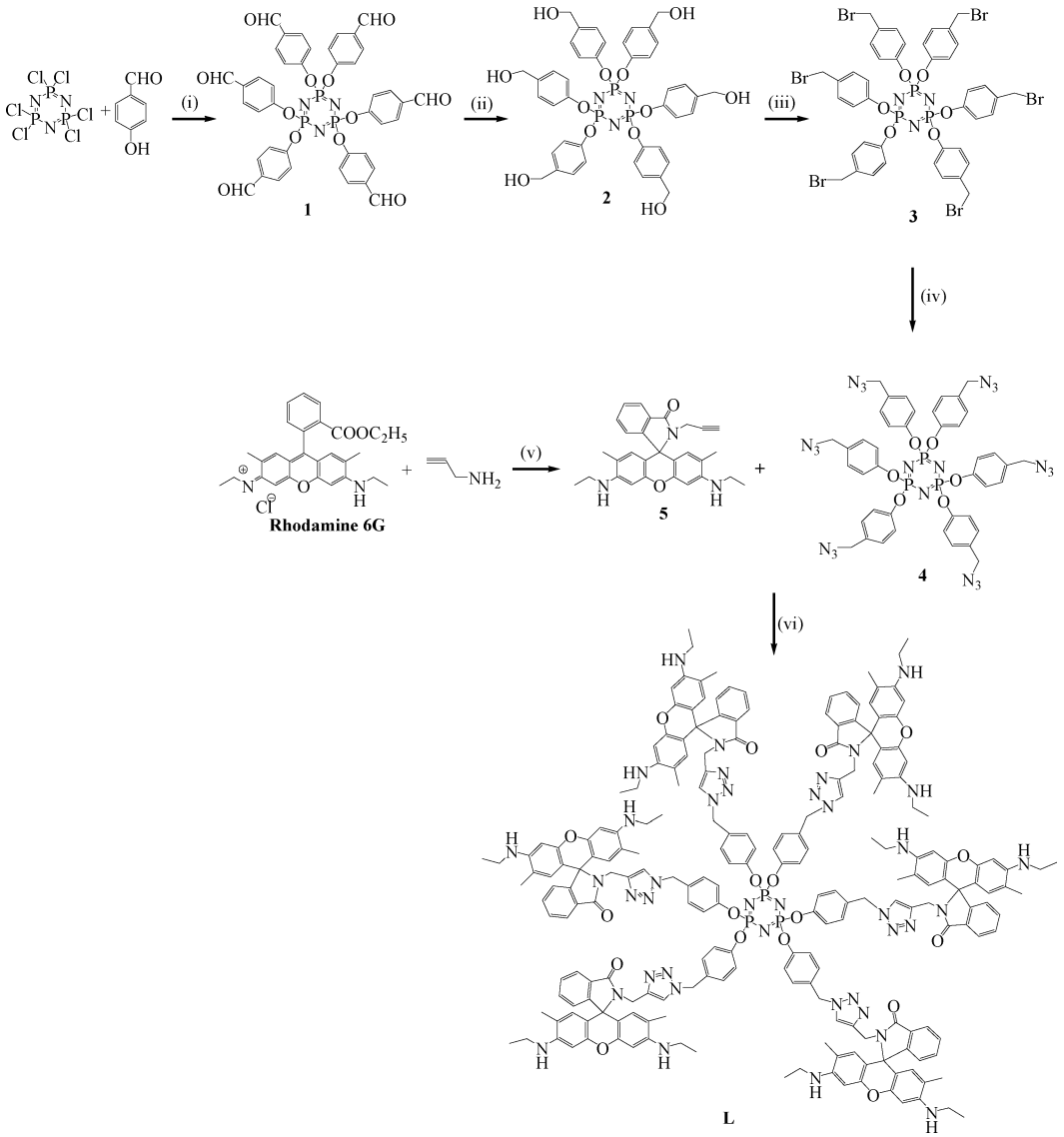

[a]Conditions: (i) Cs_2CO_3, THF, rt, 48 h; (ii) $NaBH_4$, THF/MeOH, rt, 24 h; (iii) PBr_3, THF, rt, 24 h; (iv) NaN_3, DMF, 90 °C, 24 h; (v) EtOH, reflux, 24 h; (vi) CuI, PMDETA, THF, 60 °C, 24 h.

chemosensors.[23−27] Rhodamine derivatives are colorless with a tricyclic lactam structure, and their color changes as a result of the opening of this lactam ring in the presence of an ion.[28−31] Yang et al. synthesized three rhodamine-based Fe^{3+} selective sensors, and they used these sensors for Fe^{3+} imaging in living cells.[23] In addition, Zheng et al. developed a europium-based metal−organic framework containing a terpyridine group for Fe^{3+}.[24] Recently, a few tripodal rhodamine derivatives have been reported as fluorescent sensors for Al^{3+}, Hg^{2+}, and Cu^{2+} ions.[32−34] We synthesized **L**, a new 1,2,3-triazole ring functionalized hexapodal rhodamine derivative on a cyclotriphosphazene core. We also demonstrated the sensor behavior of **L** for selective colorimetric and fluorometric detection of Fe^{3+} ion and determined the detection limit of **L** as 4.8 μM (0.27 mg L^{-1}) for Fe^{3+}.

RESULTS AND DISCUSSION

Synthesis and Characterization of Compounds. The naked-eye sensor **L** was synthesized by the "click-reaction" of azide **4** and alkyne **5** in the presence of copper(I) catalyst as shown Scheme 1 with 65% yield.

For this purpose first, compounds **4** and **5** were synthesized. Compound **1** was obtained from the reaction of hexachlorocyclotriphosphazene and 4-hydroxybenzaldehyde in the presence of Cs_2CO_3 in dry THF with 92% yield. Then, this compound was reduced to compound **2**. Compound **3** was obtained from the reaction of **2** with PBr_3 with 60.92% yield. The synthesis of azide **4** was achieved by the reaction of compound **3** and NaN_3 with 88% yield. Compound **5** was synthesized according to the literature procedure.[35] The reaction of rhodamine 6G and propargyl amine produced **5** as a pale pink solid with 68% yield.

The structures of all compounds were characterized by ^1H, ^{13}C, ^{31}P NMR; HR-MS; and MALDI-TOF MS analysis (see Experimental Section and Supporting Information Figures S1−S22). Only a singlet peak was observed in the ^{31}P NMR spectra of compounds **1**−**4** and **L**. This shows that all phosphazene compounds were fully substituted. As an example, the ^{31}P NMR

dx.doi.org/10.1021/ic402783x | Inorg. Chem. 2014, 53, 2144−2151

of **L** showed that all phosphorus atoms are identical because there is a single peak at 8.25 ppm (Supporting Information Figure S20). In the ^{1}H NMR spectrum of **L**, the signals related to protons in the triazole ring and methylene group directly attached to the nitrogen atom of the triazole ring were observed as singlets at 6.97 and 5.24 ppm, respectively (Supporting Information Figure S19).

Optical Responses of L in the Presence of Fe^{3+}. To investigate the selectivity of **L**, various cations were added to a solution of **L** in THF/H_2O (99:1, 0.01 M HEPES buffer, pH = 7.4). Rhodamine derivatives are colorless with a tricyclic lactam structure, and their color and luminescence changes as a result of the opening of this lactam ring in acidic pH. Therefore, the pH titration control experiments were carried out for free **L** and **L**–Fe^{3+} in the pH range from 1 to 12 (Supporting Information Figure S23). These experiments revealed that the solution of **L** did not show any obvious fluorescence in the pH range from 5 to 12 while the solution of **L** emits strong fluorescence in acidic media (pH = 1–4). After the addition of Fe^{3+} ions, strong fluorescence intensity was observed in the pH range from 5 to 8. Therefore, the emission measurements were carried out using HEPES as pH-controlled at pH = 7.4. In order to determine the response time of **L**, after the addition of Fe^{3+} ion the UV–vis spectra were recorded at certain time intervals and the absorption change at 532 nm was investigated (Supporting Information Figure S24). All measurements were carried out 1 h after the addition of Fe^{3+} ion because the fluorescence intensity of **L**–Fe^{3+} mixture reached equilibrium in approximately 45 min. The photostability of **L** in the absence and presence of Fe^{3+} ion was investigated for 60 min in THF/H_2O (99:1, 0.01 M HEPES buffer, pH = 7.4) (Supporting Information Figure S25). Slit width and excitation wavelength were 3 and 500 nm. The fluorescence intensity of **L** and **L**–Fe^{3+} remain the same with starting value. Therefore, it can be said that **L** and **L**–Fe^{3+} complex ion have excellent photostability.

Figure 1 represents color differences of **L** in THF/H_2O (99:1, 0.01 M HEPES buffer, pH = 7.4) upon exposure to various cation types with the same concentration. Selective binding of **L** only with Fe^{3+} is visible. In the presence of Fe^{3+} the solution color of **L** converts from colorless to pink and yellow under sunlight and UV light, respectively. However, there is no visible change in the presence of other cation types. This colorimetric difference allows the use of **L** as a color-tunable Fe^{3+} sensor for qualitative determination.

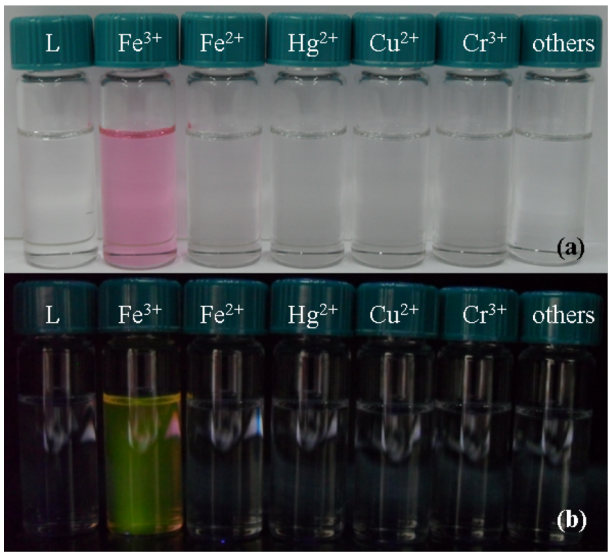

Figure 1. Solution color of **L** exposed to various types of cations under sunlight (top) and UV light (bottom).

The UV–vis spectrum recorded for **L** in THF/H_2O (99:1, 0.01 M HEPES buffer, pH = 7.4) indicated an absorption maximum at λ = 532 nm relating to the delocalized xanthane form of rhodamine group formed by opening of the spirolactam ring.[32] According to the literature, certain transition-metal ions can selectively bind with rhodamine-based molecules which results in opening of the spirolactam ring and generation of the xanthene form.[36] This conversion is determined by UV–vis and fluorescence analyses as a new band formation in the visible or NIR region.[37] A similar structural change is expected for Fe^{3+} induced **L** as shown in Figure 2. This structure for the **L**–Fe^{3+} complex was confirmed by Job's plot (see Supporting Information Figure S26a,c). The binding mechanism was also confirmed by FT-IR spectrum of **L**–Fe^{3+} complex (Supporting Information Figure S27). The characteristic C═O stretching frequency related to the amide group of the rhodamine unit was observed at 1684 cm^{-1}. This stretching frequency shifted to 1648 cm^{-1} as a shoulder in the presence of 10 equiv of Fe^{3+} ion. This shift in the frequency is the most important evidence of the binding of the rhodamine unit to Fe^{3+} ion. Similar shifts in the frequency of the C═O bond stretching related to the binding rhodamine unit to metal ions have been reported previously.[37]

Selectivity of **L** was investigated against solutions of Na^+, K^+, Ca^{2+}, Ba^{2+}, Mg^{2+}, Ag^+, Mn^{2+}, Hg^{2+}, Cu^{2+}, Ni^{2+}, Co^{2+}, Pb^{2+}, Cd^{2+}, Zn^{2+}, Fe^{2+}, Fe^{3+}, and Cr^{3+} in THF/H_2O (99:1, 0.01 M HEPES buffer, pH = 7.4). A significant absorption band formation at 532 nm is recorded for only the Fe^{3+} induced **L** solution among the tested cations (Figure 3a). Spectral changes of **L** solutions containing Fe^{3+} with various concentrations (0–50 μM) are shown in Figure 3b.

The peak values at 532 nm are plotted versus Fe^{3+} concentration (Supporting Information Figure S28a), and a linear relationship is observed with a good regression coefficient (R^2 = 0.9822) in the concentration range from 4 to 50 μM. The regression equation was A = 0.0117 [Fe^{3+}] (μM) to 0.0472. As a result, the following equation derived from the linear absorption change could be used to determine the Fe^{3+} content of any tested sample: [Fe^{3+}] (μM) = (A + 0.047)/0.012, where A is the absorbance of the sample solution. The formation of a new peak at 532 nm is attributed to the breakage of the spirolactam ring structure of **L** and subsequent formation of the xanthene form.[37]

The spectral change in emission bands could also be used in optical sensing applications. To evaluate **L** as a possible spectrofluorimetric Fe^{3+} sensor, the photoluminescence (PL) spectra were obtained. Figure 4a shows the PL spectra of **L** in THF/H_2O (99:1, 0.01 M HEPES buffer, pH = 7.4) in the absence and presence of various cations. The selective binding of **L** with Fe^{3+} among all other metal ions is visible in the PL spectra. When the **L** solution containing 50 μM Fe^{3+} is excited at 500 nm an emission band with high intensity centered at 550 nm appears. There is nearly no change in the presence of other cations. This allows the use of **L** as a selective spectrofluorometric sensor for Fe^{3+}. The quantum yield of the Fe^{3+} and **L** solution was calculated according to the comparative method and found to be 5.4%. The quantum yield of **L** in the absence of

dx.doi.org/10.1021/ic402783x | Inorg. Chem. 2014, 53, 2144–2151

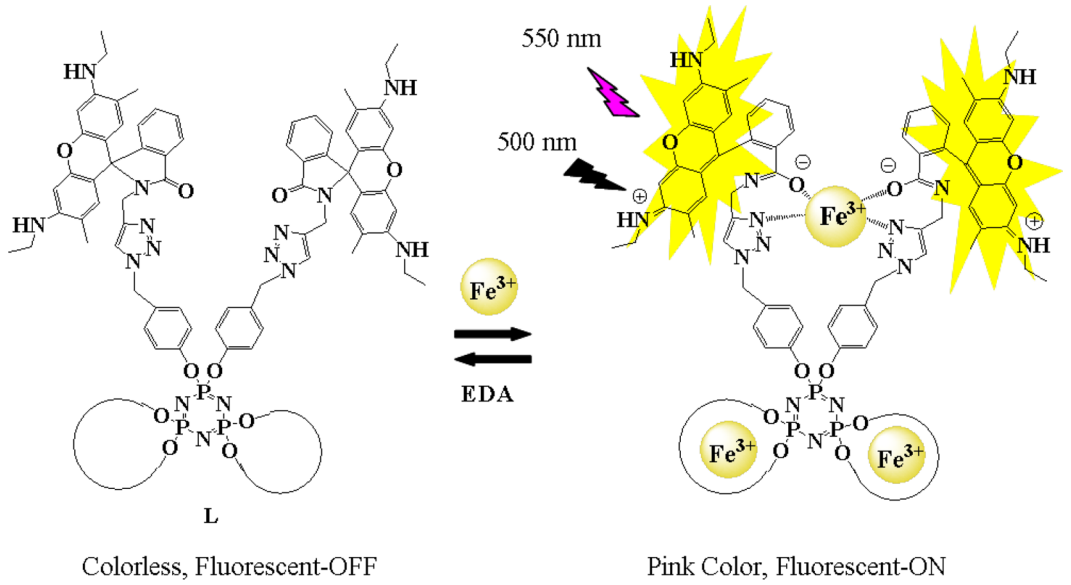

Figure 2. Proposed sensing mechanism for **L**–Fe^{3+} complex.

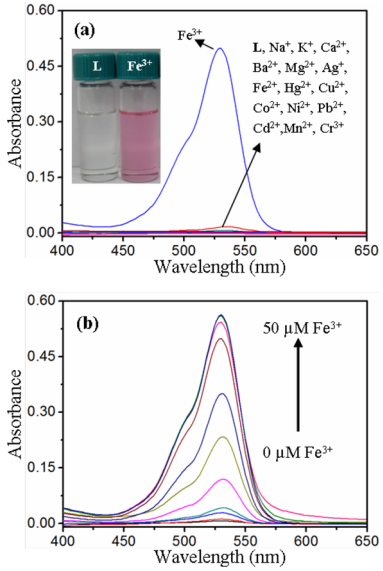

Figure 3. (a) Absorption spectra of **L** (5 μM) in the presence of different metal ions (10 equiv). Inset: The digital camera image of **L** (5 μM) and Fe^{3+} (50 μM) mixture in sunlight. (b) Absorption spectra of **L** (5 μM) upon addition of different amounts of Fe^{3+} in THF/H_2O (99:1, 0.01 M HEPES buffer, pH = 7.4).

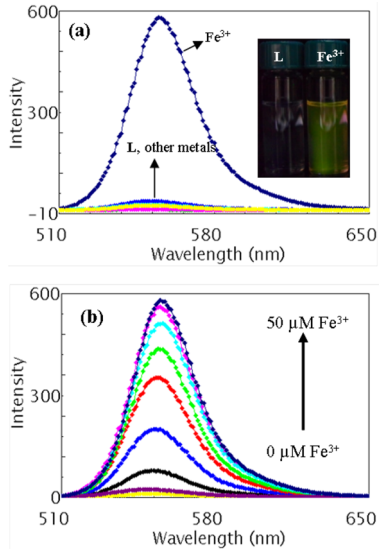

Figure 4. (a) Fluorescence spectra of **L** (5 μM) in the presence of different metal ions (10 equiv). Inset: The digital camera image of **L** (5 μM) and Fe^{3+} (50 μM) mixture at 365 nm. (b) Fluorescence intensity changes of **L** (5 μM) upon addition of different amounts of Fe^{3+} in THF/H_2O (99:1, 0.01 M HEPES buffer, pH = 7.4).

Fe^{3+} was <0.01%. This indicates a huge increase in the fluorescence band with exposure to Fe^{3+}.

A significant increase in the peak intensity at 550 nm is obtained with increasing concentration of Fe^{3+} (Figure 4b). A linear relationship is observed in the concentration range from 4 to 30 μM. The regression equation and regression coefficient were I = 20.7183 [Fe^{3+}] (μM) to 89.062 and R^2 = 0.9801, respectively. The correlation is suitable for quantitative determination of Fe^{3+}. The linear equation with a formula of [Fe^{3+}]= (I + 89.06)/20.72 is derived from the intensity change at 550 nm versus Fe^{3+} concentration (Supporting Information Figure S28b), where I is the peak intensity at 550 nm and [Fe^{3+}] is the concentration of Fe^{3+} in micromolar. Additionally, in order to determine the reproducibility or precision of the sensor, five measurements were carried out for 10 μM of Fe^{3+} under the same experimental conditions. The relative standard deviation (RSD %) was calculated as 2.2%. Thus, it may be said that the proposed sensor has high accuracy and precision.

Possible interference from other cations in the spectrofluorometric response to Fe^{3+} was tested. A series of **L** solutions, each of which simultaneously contains the same concentration of Fe^{3+} and another tested cation type, were used for testing. Figure 5 shows the changes in the intensity of the emission peak (550 nm). The peak intensity of the solution is not significantly affected by the presence of other cations indicating the presence of stable complexation between **L** and Fe^{3+}. As a result, the sensing measurement is appropriate even in the presence of high concentrations of guest metals.

To determine the stoichiometry of the **L**–Fe^{3+} complex the method of continuous variations (Job's plot) was used. The

dx.doi.org/10.1021/ic402783x | Inorg. Chem. 2014, 53, 2144–2151

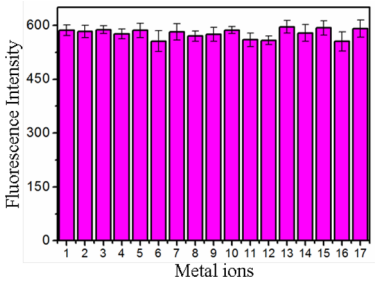

Figure 5. Fluorescence changes of the solution containing **L** and 10 equiv of Fe^{3+} upon addition of 10 equiv of competing metal ions: 1, blank (**L** + Fe^{3+}); 2, Na^{+}; 3, K^{+}; 4, Ca^{2+}; 5, Ba^{2+}; 6, Fe^{2+}; 7, Mg^{2+}; 8, Ni^{2+}; 9, Co^{2+}; 10, Zn^{2+}; 11, Cu^{2+}; 12, Hg^{2+}; 13, Mn^{2+}; 14, Cr^{3+}; 15, Cd^{2+}; 16, Ag^{+}; 17, Pb^{2+}.

stoichiometry for the **L**−Fe^{3+} complex was determined as 1:3 from Job's plot (see Supporting Information Figure S26a,c). This is also confirmed by the following equation used to calculate the stability constant for the **L**−Fe^{3+} complex (Supporting Information Figure S29).[34,38]

$$\log\left[\frac{F_{max} - F}{F - F_{min}}\right] = n \log C_M + \log K_{as}$$

Here F_{max} and F_{min} limit the fluorescence intensity at the respective wavelength, n denotes n:1 M/L stoichiometry, and K_{as} is the apparent stability constant. According to fluorescence data, stability constant and stoichiometry were calculated as 4.37×10^{14} and as approximately 3 (3.0691).[34] Additionally, the stability constant of the **L**−Fe^{3+} complex was calculated as 3.40×10^{12} from UV−vis data. The regression equation and regression coefficient were $\log[A_{max} - A/A - A_{min}] = -2.7045 \times \log[Fe^{3+}] + 12.531$ and $R^2 = 0.9816$, respectively.

The detection limit is an important parameter in sensor applications. The detection limits of **L** were calculated according to the fluorescence titration curve. A good linear relationship was obtained in the range 4−30 μM, and the detection limit of **L** was obtained as 4.8 μM (0.27 ppm) for Fe^{3+}.[38] This value is lower than the suggested water quality standards for iron ions (0.3 ppm) in drinking water by the WHO and EPA.[39,40] Several rhodamine-based sensors with 1:1 and 1:2 stoichiometry for Fe^{3+} ions are reported in the literature. For example, while the detection limit for Fe^{3+} has been reported as 100 μM by Weerasinghe et al.,[41] Chai et al.,[27] Chen et al.,[42] and Yang et al.[23] reported it to be 20, 10, and 5 μM, respectively. It may be said that **L** is a better sensor from these reported systems for Fe^{3+} due to its detection limit and 1:3 stoichiometry. Furthermore, **L**−Fe^{3+} has excellent photostability. However, a system with lower detection limit than reported here was reported by Liu and Wu (2.2 μM).[19] In the reported study, the reversibility of the sensor, the effect of competing anions on the sensing process, and the photostability of sensor and sensor−Fe^{3+} complex ion have not been investigated. Thus, there are many deficiencies of the reported system by Liu and Wu for a practical application. Our proposed rhodamine based sensor **L** is an interesting compound with hexapodal structure containing six rhodamine moieties on a cyclotriphosphazene core. Additionally, **L** has attractive features such as good photostability, high selectivity, and sensitivity.

Reversible usage is an important feature for optical chemosensors. This feature allows improvement of an on−off sensor and decreases the analysis cost. An ion exchange process by another suitable ligand is favorable for this aim. Recovery studies of **L** after complexation with Fe^{3+} were carried out using ethylenediamine (EDA).[43] The fluorescence intensity of the EDA-exposed complex solution is quenched significantly, indicating an ion exchange from **L**−Fe^{3+} complex to EDA (Figure 6). Repeated use of **L** was tested by exposure to Fe^{3+},

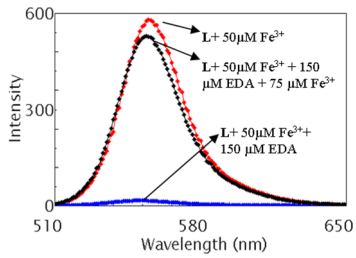

Figure 6. Reversible fluorescence response of **L** to Fe^{3+} ions.

and nearly complete recovery was obtained in the PL intensity. As a result, the present sensor is appropriate for repeated use to construct an on−off Fe^{3+} sensor.

Anions which are found in environmental samples, in addition to metal ions, can affect the detection limit of the metal ion sensor. Figure 7 shows the fluorescence intensity

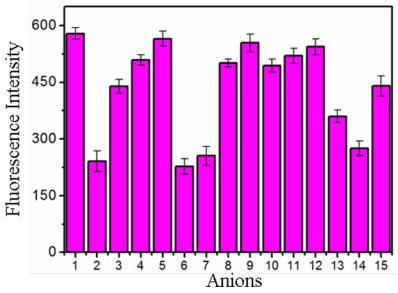

Figure 7. Fluorescence changes of the solution containing **L** and 10 equiv of Fe^{3+} upon addition of 20 equiv competing anions: 1, blank (**L** + Fe^{3+}); 2, AcO^{-}; 3, F^{-}; 4, NO_2^{-}; 5, HSO_4^{-}; 6, SCN^{-}; 7, CN^{-}; 8, Br^{-}; 9, Cl^{-}; 10, I^{-}; 11, $H_2PO_4^{-}$; 12, NO_3^{-}; 13; PO_4^{3-}; 14, CO_3^{2-}; 15, SO_4^{2-}.

changes of **L** (5 μM) and Fe^{3+} (50 μM) mixture with the addition of AcO^{-}, F^{-}, NO_2^{-}, HSO_4^{-}, SCN^{-}, CN^{-}, Br^{-}, Cl^{-}, I^{-}, $H_2PO_4^{-}$, NO_3^{-}, PO_4^{3-}, CO_3^{2-}, and SO_4^{2-} anions (100 μM). As is clearly shown in the figure, AcO^{-}, CO_3^{2-}, SCN^{-}, and CN^{-} anions cause a decrease in sensitivity of the sensor because they lead to a decrease in fluorescence intensity of the **L**−Fe^{3+} complex. However, SCN^{-} and CN^{-} anions are less common in aqueous media compared to other ions.

CONCLUSION

In this study, we report the synthesis of hexapodal **L** and its use as a naked eye fluorescent on−off sensor in the selective detection of Fe^{3+}. **L** was synthesized from the "click-reaction" of a hexaazide-substituted phosphazene compound **4** with a rhodamine 6G derivative alkyne compound **5**. It was found that **L** is an excellent selective naked eye sensor for Fe^{3+} ions in the presence of other metal ions and anions. Moreover, **L** provided remarkable fluorescence intensity and absorbance change as a result of the opening of the spirolactam ring. The complex stoichiometry of **L**−Fe^{3+} was found as 1:3 (L/M). Also, the detection limit of **L** was 4.8 μM (0.27 ppm) for Fe^{3+}.

dx.doi.org/10.1021/ic402783x | Inorg. Chem. 2014, 53, 2144−2151

EXPERIMENTAL SECTION

General Experimental Description. The reagents and all solvents except THF were purchased from chemical companies and were used without further purification. THF was dried by using Na and benzophenone. Distilled water was used in all studies. Perchlorate salts of Na^+, K^+, Ca^{2+}, Ba^{2+}, Mg^{2+}, Ag^+, Mn^{2+}, Hg^{2+}, Cu^{2+}, Ni^{2+}, Co^{2+}, Pb^{2+}, Cd^{2+}, Zn^{2+}, Fe^{2+}, Fe^{3+}, and Cr^{3+} ions; tetrabutylammonium salts of AcO^-, F^-, NO_2^-, HSO_4^-, SCN^-, CN^-, Br^-, Cl^-, I^-, HPO_4^{2-}, and NO_3^- anions; and potassium salts of PO_4^{3-}, CO_3^{2-}, and SO_4^{2-} anions were used in sensor studies. 4-(2-Hydroxyethyl)piperazine-1-ethanesulfonic acid (HEPES) was used as buffer media. All UV−vis absorption and fluorescence spectra were recorded using PG Instruments T80+ and Shimadzu RF-5301PC spectrofluorophotometer, respectively. ^{1}H, ^{13}C, and ^{31}P NMR spectra were recorded on Bruker Biospin (400 MHz) or Varian Unity INOVA (500 MHz) spectrophotometer by using tetramethylsilane and 85% H_3PO_4 as interval reference for ^{1}H NMR and ^{31}P NMR, respectively. $CDCl_3$ or DMSO-d_6 was used in all NMR measurements. Mass spectra of the compounds were recorded on Water SYNAT (HRMS ES$^+$) and Bruker Microflex LT MALDI-TOF MS spectrometers. FT-IR was recorded with a Perkin-Elmer FT-IR instrument by using an ATR apparatus with 4 cm^{-1} resolution between 4000 and 650 cm^{-1}. The analytical data of compounds were obtained using a LECO CHNS-932 elemental analyzer. Compounds **1**−**5** were similarly synthesized according to literature procedures with minor modifications.[1,2,35,44] All UV−vis absorption and fluorescence intensity measurements were repeated three times. The averaged values were given in the figures. ***Caution!*** *Metal perchlorate salts and azides are potentially explosive compounds under certain conditions such as heat, pressure, and light. Therefore, even small amounts of these compounds should be used with caution.*

Synthesis and Characterization of 1. The solution of hexachlorocyclotriphosphazene (3.48 g, 10.00 mmol) in dry THF (50 mL) was dropwise added to a magnetically stirred solution of 4-hydroxybenzaldehyde (7.46 g, 61.00 mmol) and Cs_2CO_3 (39.75 g, 121 mmol) in dry THF (200 mL) under argon atmosphere. Afterward the reaction mixture was stirred at room temperature for 48 h. At the end of this time, the insoluble salts were filtered, and the solvent was removed under reduced pressure. The white solid residue was extracted with 3 × 50 mL CH_2Cl_2. Then, the combined CH_2Cl_2 phase was extracted with 3 × 25 mL water and 3 × 25 mL brine, respectively. The organic phase was dried with Na_2SO_4. Solvent was removed under reduced pressure, and crude product was recrystallized from ethylacetate to give a white crystal solid (7.92, 92%): mp 159−160 °C. FTIR-ATR (ν_{max}, cm^{-1}): 1703 (C═O), 1584 (aromatic C═C), 1206 and 1155 (P═N), 960 (P—O—C). ^{1}H NMR (500 MHz, $CDCl_3$, 25 °C): δ 9.90 (6H, COH), 7.71 (d, Ar−H), 7.12 (d, Ar−H). ^{31}P NMR (202 MHz, $CDCl_3$, 25 °C): δ 7.04 (s). MALDI MS m/z Calcd for $C_{42}H_{30}N_3O_{12}P_3$ + (H$^+$): 862.115. Found: 862.071. Anal. Calcd for $C_{42}H_{30}N_3O_{12}P_3$: C, 58.55; H, 3.51; N, 4.88. Found: C, 58.82; H, 3.44; N, 4.91.

Synthesis and Characterization of 2. $NaBH_4$ (1.45 g, 38.28 mmol) was added to a solution of compound **1** (5.00 g, 5.80 mmol) in THF/methanol (1:1, 300 mL) mixture at room temperature. The reaction mixture was stirred for 24 h. Afterward, the solvent was evaporated, and the obtained crude solids were recrystallized to form a mixture of ethanol and water (9:1) to give compound **2** as a white solid (4.87 g, 96%): mp 218−219 °C. FTIR-ATR (ν_{max}, cm^{-1}): 3310 (O—H), 1604 (aromatic C═C), 1157 (P═N), 954 (P—O—C). ^{1}H NMR (500 MHz, DMSO-d_6, 25 °C): δ 7.18 (d, J = 7.81 Hz, 12H, ArH), 6.79 (d, J = 7.81 Hz, 12H, ArH), 5.25 (br s, 6H, CH_2OH), 4.45 (s, 12H, CH_2OH). ^{13}C NMR (125 MHz, DMSO-d_6, 25 °C): δ 149.02 (ArC), 139.83 (ArCH), 128.11 (ArCH), 120.51 (ArC), 62.69 (CH_2). ^{31}P NMR (202 MHz, DMSO-d_6, 25 °C): δ 8.84 (s). MALDI MS m/z Calcd for $C_{42}H_{42}N_3O_{12}P_3$ + (H$^+$): 874.205. Found: 874.265. Anal. Calcd for $C_{42}H_{42}N_3O_{12}P_3$: C, 57.74; H, 4.85; N, 4.81. Found: C, 57.44; H, 4.91; N, 4.72.

Synthesis and Characterization of 3. To a solution of **2** (4.00 g, 4.58 mmol) in dry THF was added dropwise phosphorus tribromide (10.00 g, 18.47 mmol) via a syringe through the septum at −10 °C. The reaction mixture was magnetically stirred at room temperature for 24 h. The solvent was removed by rotary evaporator and to the viscose oily residue was added distilled water (250 mL). The resulting white precipitate was collected by filtration and washed with distilled water until neutral. The crude product was purified by column chromatography on silica gel with $CHCl_3$/hexane (4:1) solvent mixture to give **3** as a white crystal solid (3.49 g, 60.92%): mp 149−150 °C. FTIR-ATR (ν_{max}, cm^{-1}): 1602 (aromatic C═C), 1264 and 1159 (P═N), 952 (P—O—C). ^{1}H NMR (500 MHz, $CDCl_3$, 25 °C): δ 7.25 (d, J = 8.54 Hz, 12H, ArH), 6.90 (d, J = 8.54 Hz 12H, ArH), 4.48 (s, 6H, CH_2Br). ^{13}C NMR (125 MHz, $CDCl_3$, 25 °C): δ 150.18 (ArC), 134.51 (ArC), 130.27 (ArCH), 121.23 (ArCH), 32.91 (CH_2). ^{31}P NMR (202 MHz, $CDCl_3$, 25 °C): δ 8.51 (s). MALDI MS m/z Calcd for $C_{42}H_{36}Br_6N_3O_6P_3$: 1251.105. Found: 1251.415. Anal. Calcd for $C_{42}H_{36}Br_6N_3O_6P_3$: C, 40.32; H, 2.90; N, 3.36. Found: C, 40.85; H, 2.85; N, 3.64.

Synthesis and Characterization of 4. The solution of **3** (3.00 g, 2.40 mmol) and NaN_3 (1.56 g, 24.00 mmol) in DMF (10 mL) was heated at 90 °C for 24 h under argon atmosphere. At the end of this time, the reaction mixture was cooled to room temperature and poured into rapidly magnetically stirred distilled water (200 mL). The mixture was stirred for 15 min, and the resulting solid was collected by filtration. Afterward, the dried solid was isolated as white solid by column chromatography on silica gel with EtOAc/hexane (3:7) solvent mixture (2.16 g, 88%): mp 125−126 °C. FTIR-ATR (ν_{max}, cm^{-1}): 1605 (aromatic C═C), 1264 and 1177 (P═N), 959 (P—O—C). ^{1}H NMR (500 MHz, $CDCl_3$, 25 °C): 7.16 (d, J = 8.46 Hz, 12H, ArH), 6.97 (d, J = 8.46 Hz, 12H, ArH), 4.32 (s, 12H; CH_2N_3). ^{13}C NMR (125 MHz, $CDCl_3$, 25 °C): δ 150.36 (ArC), 132.11 (ArCH), 129.35 (ArCH), 121.23 (ArC), 54.12 (CH_2N_3). ^{31}P NMR (202 MHz, $CDCl_3$, 25 °C): δ 8.41 (s). MALDI MS m/z Calcd for $C_{42}H_{36}N_{21}O_6P_3$ + (H$^+$): 1024.244. Found: 1024.431. Anal. Calcd for $C_{42}H_{36}N_{21}O_6P_3$: C, 49.27; H, 3.54; N, 28.73. Found: C, 49.43; H, 3.48; N, 28.81.

Synthesis and Characterization of 5. To a solution of rhodamine 6G (2.40 g, 5.00 mmol) in methanol (25 mL) was added propargyl bromide (1.60 mL, 25.00 mmol), and the reaction mixture was refluxed for 24 h. After the evaporation of the solvent, the dark red residue was purified by column chromatography on silica gel with CH_2Cl_2/hexane solvent mixture to give a pale pink solid (1.54 g, 68%): mp 253−254 °C. FTIR-ATR (ν_{max}, cm^{-1}): 3442 and 3278 (N—H), 1700 (C═O). ^{1}H NMR (300 MHz, DMSO-d_6, 25 °C): 7.81 (m, 1H), 7.49 (m, 1H), 6.98 (m, 1H), 6.27 (s, 2H), 6.13 (s, 2H), 5.06 (s, 2H), 3.77 (s, 2H), 3.13 (m, 4H), 2.69 (s, 1H), 1.87 (s, 6H), 1.21 (m, 6H). ^{13}C NMR (75 MHz, DMSO-d_6, 25 °C): δ 166.91 (C═O), 154.37, 151.57, 148.17, 133.43, 129.93, 128.73, 128.26, 124.05, 122.96, 118.51, 104.32, 96.32, 79.33 (Ar—C), 73.05 (*C*≡CH), 64.79 (C≡*CH*), 37.96 and 28.61 (N—CH_2), 17.52 and 14.63 (CH_3). HRMS (ES$^+$) m/z Calcd for $C_{29}H_{29}N_3O_2$ + (Na$^+$): 474.196. Found: 474.197. Anal. Calcd for $C_{29}H_{29}N_3O_2$: C, 77.13; H, 6.47; N, 9.31. Found: C, 76.90; H, 3.51; N, 9.36.

Synthesis and Characterization of L. To a solution of compound **4** (0.1024 g, 0.10 mmol) and compound **5** (0.32 g, 0.72 mmol) in dry THF (25 mL) was added *N*,*N*,*N*′,*N*″,*N*″-pentamethyldiethylenetriamine (PMDETA, 0.25 mL, 1.20 mmol), and the solution was purged with argon for 15 min. Afterward, copper(I)iodide (0.0114 g, 0.06 mmol) was added to the reaction mixture. The mixture was degassed with argon, and it was stirred at 60 °C for 24 h under argon atmosphere. At the end of this time, the reaction mixture cooled to room temperature, and the solvent was evaporated under reduced pressure. The residue was purified by column chromatography on silica gel with $CHCl_3$/methanol (9:1) solvent mixture to give a pale orange solid (0.24 g, 65%): mp 235−237 °C. FTIR-ATR (ν_{max}, cm^{-1}): 3377 (N—H), 1683 (C═O), 1198 and 1159 (P═N), 952 (P—O—C). ^{1}H NMR (300 MHz, $CDCl_3$, 25 °C): 7.88 (m, 6H), 7.41 (m, 12H), 7.06 (m, 6H), 6.97 (m, 6H), 6.85 (d, J = 8.60 Hz, 12H), 6.75 (d, J = 8.60 Hz, 12H), 6.30 (s, 12H), 6.07 (s, 12H), 5.24 (s, 12H), 4.42 (s, 12H), 3.68 (b, 12 H), 3.18 (q, J = 6.95 Hz, 24H), 1.78 (s, 36H), 1.28 (t, J = 6.95 Hz, 36H). ^{13}C NMR (75 MHz, $CDCl_3$, 25 °C): δ 167.94 (C═O), 153.67, 151.76, 150.04, 147.39, 144.47, 132.61,

dx.doi.org/10.1021/ic402783x | *Inorg. Chem.* 2014, 53, 2144−2151

132.11, 130.71, 128.85, 128.47, 128.06, 123.84, 122.88, 121.02, 117.76, 105.39, 96.41, 65.16, 52.65, 64.79, 38.31, 35.14, 16.64, 14.71. ^{31}P NMR (202 MHz, DMSO-d_6, 25 °C): 8.25. MALDI MS m/z Calcd for $C_{216}H_{210}N_{39}O_{18}P_3$: 3729.397 Found: 3729.400. Anal. Calcd for $C_{216}H_{210}N_{39}O_{18}P_3$: C, 69.49; H, 5.67; N, 14.63. Found: C, 69.27; H, 5.61; N, 14.69.

UV−Vis Absorption Experiments. The stock solutions of **L** and metal ions were prepared in THF/H_2O (99:1, 0.01 M HEPES buffer, pH = 7.4). All spectra were measured at 25 °C in this solvent mixture. During the measurements, stock solutions of **L** and metal ions were added into 3 mL of THF/H_2O (99:1, 0.01 M HEPES buffer, pH = 7.4) mixture by using a micropipet. In order to keep a constant concentration of the test solutions, the total volume of the added stock solutions was maintained at less than 100 μL.

Fluorescence Measurements. Fluorescence characteristics were determined by a Shimadzu RF-5301PC spectrofluorophotometer. Measurements were carried out using THF/H_2O (99:1, 0.01 M HEPES buffer, pH = 7.4) solutions of **L**. The effects of transition metal ions on selectively quenching−growing of the emission spectra were investigated in solutions each of which contained 5 μM of **L** and 50 μM metal ions. The change of fluorescence intensities depending on the concentration of Fe^{3+} was determined using a series of different concentration Fe^{3+} solutions. Possible interference from other cation types was investigated using separate solutions of **L**, each of which simultaneously contained Fe^{3+} and another cation with excess concentration. Reversibility of the sensor was tested using ethylene diamine (EDA) as a guest ligand for ion exchange. Slit width and excitation wavelength were 3 and 500 nm in all experiments. Fluorescence quantum yield (QY) is calculated by comparative methods using rhodamine 6G solution in ethanol as the standard. The calculation was carried out as described in the literature by the following equation[45,46]

$$QY_X = QY_S \times [A_X/A_S] \times [F_S/F_X] \times [n_X/n_S]^2$$

where QY_X and QY_S are the quantum yields of the sample and the standard, A_X and A_S are the integrated peak areas under the corrected fluorescence spectra of the sample and the standard. F_S and F_X are fractions of light absorbed by the standard and the sample determined by the following equation: $F = 1-10^{-D}$, where D is the optical density (absorbance) at the excitation wavelength. n_X and n_S are the refractive indexes of the solvents used.

■ ASSOCIATED CONTENT

Ⓢ Supporting Information

^{1}H, ^{13}C, and ^{31}P NMR spectra, and HRMS and MALDI-MS spectra of all intermediates and **L**. Fluorescence spectra, FT-IR spectra of **L** and **L**−Fe^{3+} complex, Job plots, detection limits, and apparent stability constant determination. This material is available free of charge via the Internet at http://pubs.acs.org.

■ AUTHOR INFORMATION

Corresponding Author

*E-mail: havaozay@comu.edu.tr.

Notes

The authors declare no competing financial interest.

■ ACKNOWLEDGMENTS

This work was financially supported by the Scientific and Technological Research Council of Turkey (TUBITAK, Project 112T278).

■ REFERENCES

(1) Gorur, M.; Yilmaz, F.; Kilic, A.; Sahin, Z. M.; Demirci, A. *J. Polym. Sci., Part A: Polym. Chem.* **2011**, *49*, 3193−3206.

(2) Gorur, M.; Yımaz, F.; Kilic, A.; Demirci, A.; Ozdemir, Y.; Kosemen, A.; San, E. A. *J. Polym. Sci., Part A: Polym. Chem.* **2010**, *48*, 3668−3682.

(3) Tian, Z.; Chen, C.; Allcock, H. R. *Macromolecules* **2013**, *46*, 2715−2724.

(4) Allcock, H. R. *Appl. Organometal. Chem.* **2013**, *27*, 620−629.

(5) Davidson, R. J.; Ainscough, E. W.; Brodie, A. M.; Jameson, G. B.; Waterland, M. R.; Allcock, H. R.; Hindenlang, M. D.; Moubaraki, B.; Murray, K. S.; Gordon, K. C.; Horvath, R.; Jameson, G. N. L. *Inorg. Chem.* **2012**, *51*, 8307−8316.

(6) Alidagi, H. A.; Girgic, O. M.; Zorlu, Y.; Hacivelioglu, F.; Celik, S. U.; Bozkurt, A.; Kilic, A.; Yesilot, S. *Polymer* **2013**, *54*, 2250−2256.

(7) Allen, C. W. *Chem. Rev.* **1991**, *91*, 119−135.

(8) Cosut, B.; Yesilot, S. *Polyhedron* **2012**, *35*, 101−107.

(9) Bai, Y.; Wang, X.; Wu, D. *Ind. Eng. Chem. Res.* **2012**, *51*, 15064−15074.

(10) Jiménez, J.; Laguna, A.; Gascón, E.; Sanz, J. A.; Serrano, J. L.; Barberá, J.; Oriol, L. *Chem.—Eur. J.* **2012**, *18*, 16801−16814.

(11) Yildirim, T.; Bilgin, K.; Ciftci, G. Y.; Ecik, E. T.; Senkuytu, E.; Uludag, Y.; Tomak, L.; Kilic, A. *Eur. J. Med. Chem.* **2012**, *52*, 213−220.

(12) Liu, X.; Zhang, H.; Tian, Z.; Sen, A.; Allcock, H. R. *Polym. Chem.* **2012**, *3*, 2082−2091.

(13) Nichol, J. L.; Morozowich, N. L.; Allcock, H. R. *Polym. Chem.* **2013**, *4*, 600−606.

(14) Deng, M.; Nair, L. S.; Nukavarapu, S. P.; Jiang, T.; Kanner, W. A.; Li, X.; Kumbar, S. G.; Weikel, A. L.; Krogman, N. R.; Allcock, H. R.; Laurencin, C. T. *Biomaterials* **2010**, *31*, 4898−4908.

(15) Ainscough, E. W.; Brodie, A. M.; Edwards, P. J. B.; Jameson, G. B.; Otter, C. A.; Kirk, S. *Inorg. Chem.* **2012**, *51*, 10884−10892.

(16) Badetti, E.; Lloveras, V.; Wurst, K.; Sebastian, R. M.; Caminade, A. M.; Majoral, J. P.; Veciana, J.; Vidal-Gancedo, J. *Org. Lett.* **2013**, *15*, 3490−3493.

(17) Keller, M.; Colliere, V.; Reiser, O.; Caminade, A. M.; Majoral, J. P.; Ouali, A. *Angew. Chem., Int. Ed.* **2013**, *52*, 3626−3629.

(18) Caminade, A. M.; Majoral, J. P. *New J. Chem.* **2013**, *37*, 3358−3373.

(19) Liu, S. R.; Wu, S. P. *Sens. Actuators, B* **2012**, *171−172*, 1110−1116.

(20) Weerasinghe, A. J.; Schmiesing, C.; Varaganti, S.; Ramakrishna, G.; Sinn, E. *J. Phys. Chem. B* **2010**, *114*, 9413−9419.

(21) Bhalla, V.; Sharma, N.; Kumar, N.; Kumar, M. *Sens. Actuators, B* **2013**, *178*, 228−232.

(22) Zhang, L.; Wang, J.; Fan, J.; Guo, K.; Peng, X. *Bioorg. Med. Chem. Lett.* **2011**, *21*, 5413−5416.

(23) Yang, Z.; She, M.; Yin, B.; Cui, J.; Zhang, Y.; Sun, W.; Li, J.; Shi, Z. *J. Org. Chem.* **2012**, *77*, 1143−1147.

(24) Zheng, M.; Tan, H.; Xie, Z.; Zhang, L.; Jing, X.; Sun, Z. *ACS Appl. Mater. Interfaces* **2013**, *5*, 1078−1083.

(25) Li, Z. X.; Zhou, W.; Zhang, L. F.; Yuan, R. L.; Liu, X. J.; Wei, L. H.; Yu, M. M. *J. Lumin.* **2013**, *136*, 141−144.

(26) She, M.; Yang, Z.; Yin, B.; Zhang, J.; Gu, J.; Yin, W.; Li, J.; Zhao, G.; Shi, Z. *Dyes Pigm.* **2012**, *92*, 1337−1343.

(27) Chai, M.; Zhang, D.; Wang, M.; Hong, H.; Ye, Y.; Zhao, Y. *Sens. Actuators, B* **2012**, *174*, 231−236.

(28) Yan, F.; Wang, M.; Cao, D.; Yang, N.; Fu, Y.; Chen, L. *Dyes Pigm.* **2013**, *98*, 42−50.

(29) Zhang, D.; Li, M.; Wang, M.; Wang, J.; Yang, X.; Ye, Y.; Zhao, Y. *Sens. Actuators, B* **2013**, *177*, 997−1002.

(30) Sreenath, K.; Clark, R. J.; Zhu, L. *J. Org. Chem.* **2012**, *77*, 8268−8279.

(31) Huang, J.; Xu, Y.; Qian, X. *J. Org. Chem.* **2009**, *74*, 2167−2170.

(32) Maity, S. B.; Bharadwaj, P. K. *Inorg. Chem.* **2013**, *52*, 1161−1163.

(33) Zeng, X.; Dong, L.; Wu, C.; Mu, L.; Xue, S. F.; Tao, Z. *Sens. Actuators, B* **2009**, *141*, 506−510.

(34) Jana, A.; Kim, J. S.; Jung, H. S.; Bharadwaj, P. K. *Chem. Commun.* **2009**, 4417−4419.

(35) Wu, J. S.; Hwang, I. C.; Kim, K. S.; Kim, J. S. *Org. Lett.* **2007**, *9*, 907−910.

(36) Chen, X.; Pradhan, T.; Wang, F.; Kim, J. S.; Yoon, J. *Chem. Rev.* **2012**, *112*, 1910−1956.
(37) Kar, C.; Adhikari, M. D.; Ramesh, A.; Das, G. *Inorg. Chem.* **2013**, *52*, 743−752.
(38) Wang, J.; Lin, W.; Yuan, L.; Song, J.; Gao, W. *Chem. Commun.* **2011**, *47*, 12506−12508.
(39) World Health Organization. Water safety plans. In *WHO Guidelines for Drinking Water Quality*, 4th ed.; WHO: Geneva, 2011; p 226; http://whqlibdoc.who.int/publications/2011/9789241548151_eng.pdf.
(40) United States Environmental Protection Agency. *National Primary Drinking Water Regulations*; EPA 816-F-09-0004; EPA: Washington, DC, 2009; http://www.epa.gov/safewater/.
(41) Weerasinghe, A. J.; Abebe, F. A.; Sinn, E. *Tetrahedron Lett.* **2011**, *52*, 5648−5651.
(42) Chen, X.; Hong, H.; Han, R.; Zhang, D. *J. Fluoresc.* **2012**, *22*, 789−794.
(43) Yin, W.; Cui, H.; Yang, Z.; Li, C.; She, M.; Yin, B.; Li, J.; Zhao, G.; Shi, Z. *Sens. Actuators, B* **2011**, *157*, 675−680.
(44) Touaibia, M.; Roy, R. *J. Org. Chem.* **2008**, *73*, 9292−9302.
(45) Williams, A. T. R.; Winfield, S. A.; Miller, J. N. *Analyst* **1983**, *108*, 1067−1071.
(46) Lakowicz, J. R. *Principles of Fluorescence Spectroscopy*, 2nd ed.; Kluwer Academic/Plenum Publishers: New York, 1999.